A Highly Efficient Dual-band Harmonic-tuned GaN RF Synchronous Rectifier with Integrated Coupler and Phase Shifter

Md Aminul Hoque[#1], Sheikh Nijam Ali[$#], Mohammad Ali Mokri[#], Srinivasan Gopal[*#], Mohammad Chahardori[#], Deukhyoun Heo[#]
[#]Dept. of EECS, Washington State University, Pullman, WA, USA
[$]Skyworks Solutions, Inc., San Jose, CA, USA
[*]Intel Corporation, Hillsboro, OR, USA
[1]mdaminul.hoque@wsu.edu

***Abstract*— This paper presents a dual-band RF rectifying circuit for wireless power transmission at 1.17 GHz and 2.4 GHz. A dual-band harmonic-tuned inverse-class F/class-F mode power amplifier using a 10 W GaN device has been utilized to implement the proposed rectifier with an on-board coupler and phase shifter. The matching circuit is precisely designed so that the circuit operates in inverse class F and class F mode in the lower and upper frequency bands using dual-band harmonic tuning, respectively. Measurement results show that the rectifier circuit has 78% and 76% efficiencies at 1.17 GHz and 2.4 GHz frequency bands, respectively. To the best of the authors' knowledge, this rectifier is the first demonstration of a dual-band harmonic-tuned synchronous rectifier using a GaN HEMT device with an integrated coupler and phase-shifter for a watt-level RF input power.**

***Keywords*—wireless power transmission, wireless charging, high power, RF synchronous rectifiers, integrated coupler, phase-shifter, GaN HEMT device, dual-band, power amplifiers, class-F, inverse class-F.**

I. Introduction

Highly efficient RF rectifier circuits with high-power handling capability are critical to meet the unprecedented demand for high-power wireless charging/harvesting systems in many important electronic devices such as cell-phones, drones, etc [1]. Many works can be found in literature based on Schottky diode rectifiers, however, their power handling capability is not adequate for high RF input power levels [2]. Synchronous rectifier using GaN HEMT devices is an effective way to address the high-power rectifier circuits at RF frequencies.

At the same time, multi-band rectifier circuits are essential for next-generation wireless charging systems because it can support multi-band communications thus reducing the size, cost and design complexity. Several high efficiency synchronous rectifiers have been demonstrated using GaN HEMT devices employing time reversal duality [3]–[5]. However, multi-band operation for such rectifiers for high input RF powers has not been presented before. Moreover, most of the previous works employ an off-shelf coupler and an off-shelf phase-shifter to generate the appropriate gate signal for the rectifier [3], [5], [6], which increases the overall size. As a result, there is a clear need for multi-band fully-integrated high-power high-efficiency RF synchronous rectifier for next-generation wireless charging systems.

In this work, we propose for the first time a dual-band harmonic-tuned synchronous rectifier using a GaN HEMT device with an integrated coupler and phase-shifter for a watt-level RF input power. A compact harmonic-tuned dual-band load network is proposed which concurrently satisfy an inverse class-F and class-F load characteristics at 1.17 and 2.4GHz, respectively. Experimental results using a 10W Cree GaN HEMT device show that the rectifier circuit has >76% peak efficiencies at both frequency bands.

II. Proposed Dual-Band Synchronous Rectifier Circuit

Fig. 1 shows a circuit diagram of the proposed dual-band harmonic-tuned synchronous rectifier. We used C_b as a DC blocking capacitor and L_d as an RF choke. A resistor R_{gg} is used for gate biasing and a small damping resistor R_{damp} is used at the gate terminal for improved stability.

The proposed output matching circuit of the rectifier works as an inverse class-F and a class-F harmonic load network at low-band and high-band, respectively. The separation of the frequency bands is one octave. We used two open stub microstrip lines (TL2 and TL5) and two series microstrip lines (TL3 and TL4) to achieve the required harmonic load conditions for both bands concurrently.

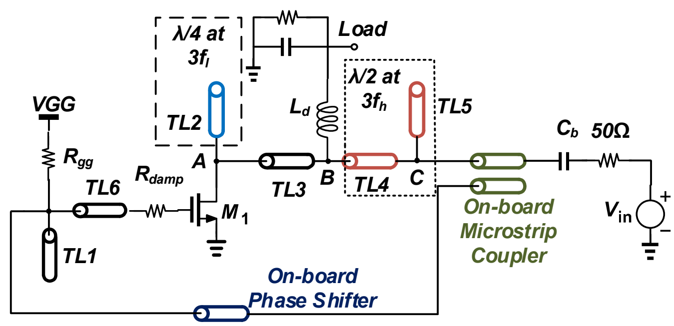

Fig. 1. The proposed dual-band harmonic-tuned synchronous rectifier with an integrated coupler and phase-shifter.

To derive the gate signal from the RF input of the rectifier, an integrated microstrip coupler is proposed. This coupler is designed as a pair of coplanar microstrip coupled lines with one open termination. By maintaining suitable gap between the coupled lines, the coupler can transmit required gate drive input power for the rectifier. The proposed coupler has a wideband frequency response and is capable to cover both low and high frequency bands, simultaneously. Further, the insertion loss is relatively low at both bands due to its small form factor and better impedance matching. The width of the line is 1.33 mm and the length is 14.85 mm. The separation between the two lines is 180 μm. The magnitude response of the coupler obtained from ADS Momentum simulation is depicted in Fig. 2. At 1.17 GHz, the coupling co-efficient is -21.6 dB and at 2.4 GHz it is -16 dB. The insertion loss in both bands are 0.1 dB and 0.2 dB, respectively. Low-loss is achieved due to the small size of the coupler.

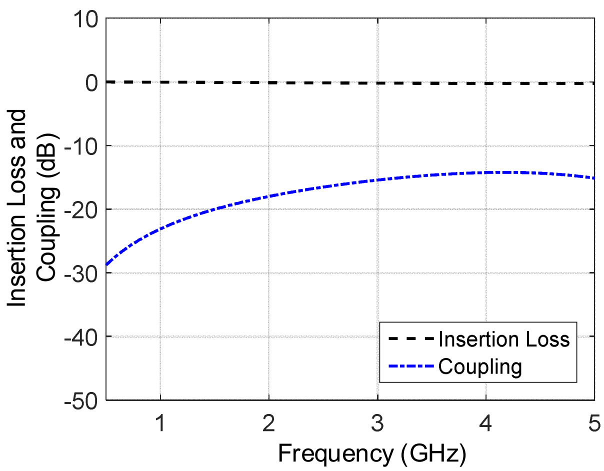

Fig. 2. Frequency response (simulation) of the on-board coupler, which shows low insertion loss across wide frequency range.

Since the gate signal is derived from the RF input signal through a coupler and phase shifter, the signal phase needs to be adjusted for proper operation of the rectifier circuit. This condition is critical to achieve high rectification efficiency since any deviation from the desired phase-shift can alter the expected performance. Many previous works employ external phase shifter for this purpose [3], [5]. However, external phase shifter creates potential impedance mismatches, compromising performances.

In this work, we propose an integrated microstrip line-based phase-shifter, which removes the added complexity of external phase-shifters. The integrated phase shifter eliminates inter-stage matching issues between the coupler and the phase-shifter. Since required gate signal is derived directly from the input RF signal in a fully-integrated approach, a proper synchronous or self-driving mode can be assured, thus ensuring high performances.

The output matching network provides fundamental matching at $f_l = 1.17\,GHz$ and $f_h = 2.4\,GHz$. Load-pull simulation is performed and optimum load impedance at fundamental frequencies are found as:

$$Z_{opt(f_l)} = (30.46 + j26)\ \Omega$$

$$Z_{opt(f_h)} = (13.8 + j28.9)\ \Omega.$$

TL2 is an open-ended stub which is $\lambda/4$ at the third harmonic of f_l and provides a short termination for $3f_l$ at node A. The second harmonic open termination is not used in this circuit as it is very close to 2.4 GHz. The odd harmonic short termination makes the circuit act in an inverse class-F mode. On the other hand, TL3 is designed to be $\lambda/2$ at $3f_h$, which makes same impedance at node A and B at this frequency. The other two sections TL4 and TL5 are used to provide $\lambda/2$ at $3f_h$, which ultimately makes an open termination at node A at $3f_h$. Therefore, the circuit operates in class-F mode in this frequency. Finally, the lengths are adjusted to provide the fundamental load impedances at the two bands. The lengths were further tuned to obtain maximum efficiency from the rectifier circuit. The physical dimensions of the transmission lines are enlisted in Table 1.

Table 1. Physical Dimensions of the Microstrip Lines

TLine	TL1	TL2	TL3	TL4	TL5	TL6
Length (mm)	6.56	6.4	12.83	4.3	3.2	7.4
Width (mm)	2.16	2.03	5	1.8	3.4	1.4

Using these parameters, the drain matching circuit is designed and simulated. The impedances at the fundamentals and harmonics seen from the drain node of the device are shown in the smith chart (Fig. 3).

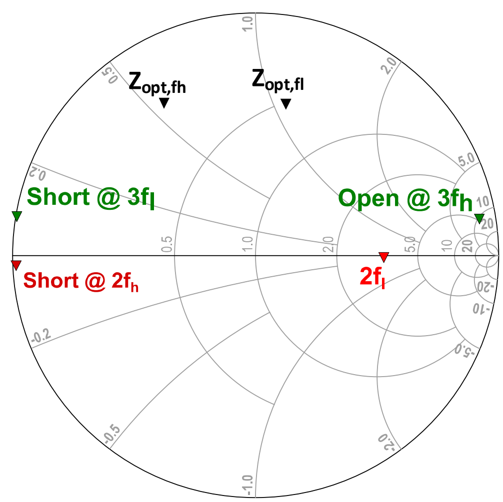

Fig. 3. Smith chart representation showing impedances at fundamentals and harmonics of the two bands at the drain node.

III. Implementation and Experimental Results

To demonstrate proposed dual-band harmonic-tuned rectifier, a Rogers 20 mil 4350B substrate with dielectric constant of 3.66 and low dissipation factor (tanδ = 0.003) is used. Further, a 10W Cree GaN-HEMT (CGH40010F) is used as the active device. Other passive components include high-Q compact size chip inductors from Coilcraft (0603CS) and ceramic capacitors from ATC (600S27). An external drive amplifier from Cree (CGH27015-TB) with a Keysight signal generator (E8257D) is used to generate required input power to test the rectifier circuit. A directional coupler with spectrum analyzer is used to observe and adjust the input power (P_{in}) to the rectifier.

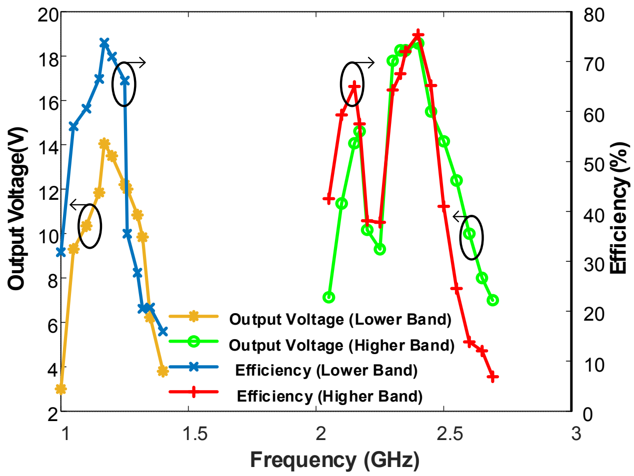

Fig. 4. Measured efficiency and output DC voltage vs. frequency plot (only the frequencies around 1.17GHz and 2.4 GHz are shown)

Fig. 4 shows the measured output voltage and efficiency obtained from the rectifier circuit. The drain efficiency is considered to be the rectification efficiency ($\eta_{rect\%}$) in this measurement, which is expressed by:

$$\eta_{rect\%} = \frac{V_{DC}^2}{R_{DC} \times P_{in}} \times 100\ \% \qquad (1)$$

Here, V_{DC} is the output DC voltage across the load R_{DC}. As shown in Fig. 4, there are two distinct peaks in efficiency, which shows the dual-band operation of the circuit. The bias condition for this measurement is kept as follows: V_{gg} = -5V, $P_{RF,in} = 40\ dBm$. The DC load resistance is kept constant at 50Ω. Measurement results show that at 2.4 GHz, output DC power reaches 7.18 W for 9.5 W input, making the efficiency 75.5% as shown in Fig. 5. The efficiency remains above 50% even when input power is 32 dBm (~1.5 W), which shows good efficiency at the back-off input power region.

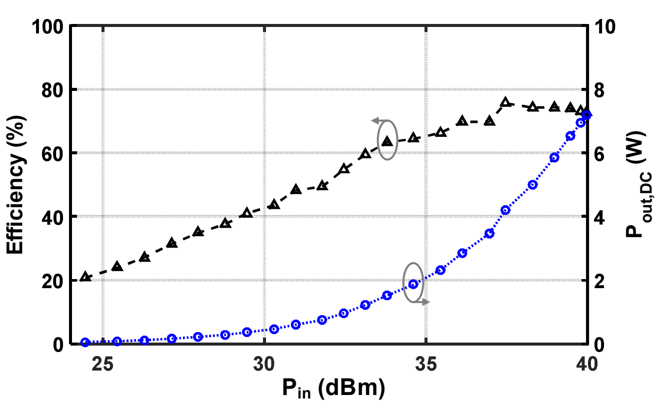

Fig. 5. Measured efficiency and output DC power vs. input power at 2.4 GHz.

For the low band, peak efficiency is reached 78% at input power of 38.2 dBm. The DC power at this level is 5.1 W. A 40 dBm input power at 1.17 GHz could not be achieved because this frequency band was out of range for the driver. But the overall trend at this frequency shows good agreement with the previously reported class-F^{-1} rectifier [3]. An input power sweep at this frequency is shown in Fig. 6, where the output DC power and efficiency is reported. It shows higher input power range compared to the 2.4 GHz operation, which is expected since at 2.4 GHz, the rectifier operates in class-F mode, whereas it operates in inverse class-F mode at 1.17 GHz [3]. The input power range is higher in this mode, as it maintains at least 50% efficiency for 25 dBm input power.

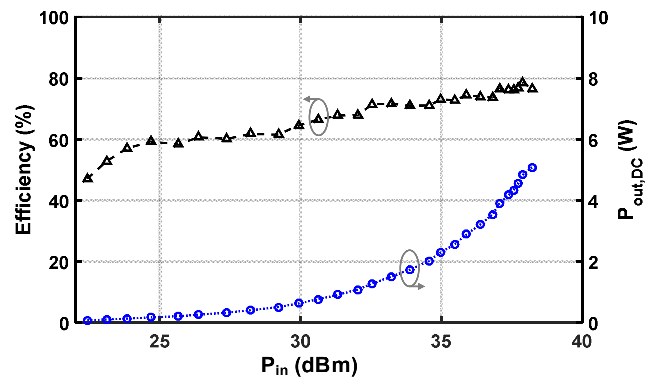

Fig. 6. Measured efficiency and output DC power vs. input power at 1.17 GHz.

The output DC voltage at 50 Ω obtained at 2.4 GHz is 18.9 V. The voltage varies with changing load, while keeping the output DC power constant. In the 1.17 GHz band, the optimum load impedance is found to be 35 Ω. Fig. 7 shows a photo of the fabricated board of the circuit. The dimension of the board is 5.2 cm x 5 cm.

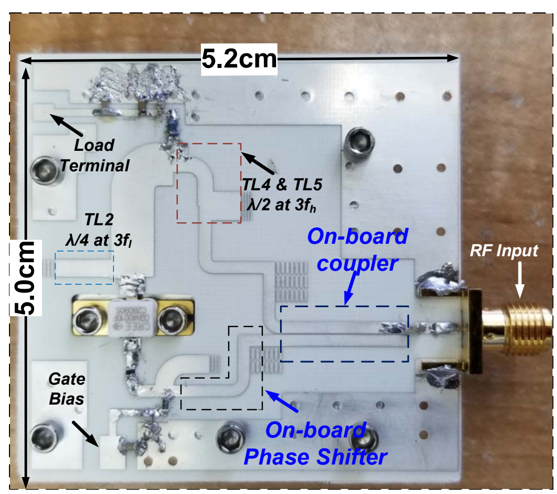

Fig. 7. Photo of the fabricated dual-band harmonic-tuned synchronous rectifier circuit.

A comparison with prior arts is provided in Table 2. Although dual-band rectifiers have been demonstrated before, most of the designs are designed using Schottky diodes [7] and no harmonic tuning for high RF input power applications.

Table 2. Summary of Synchronous RF Rectifiers

Ref.	Freq. (GHz)	P_{in} (W)	Effi. (%)	Device	Matching type	Class
[5]	1.8	10	77	GaN	Harmonic tuning	Class-F^{-1}
[6]	10.1	3.18	63.9	GaN MMIC	Passive tuning	Class-C
[8]	2.8	10	70.8	GaN	Harmonic tuning	Class-E
[7]	2.45/ 5.8	0.01	66.8/ 51.5	Schottky diode	No harmonic tuning	-
This work	**1.17/ 2.4**	**10**	**78/ 76**	**GaN**	Dual-band harmonic tuning	**Class-F^{-1}/ Class F**

IV. Conclusion

This paper presents a dual-band harmonic-tuned synchronous RF rectifier with integrated coupler and phase-shifter with high-power handling capability for the first time. The proposed rectifier can operate at two distinct octave frequency bands, 1.17 GHz and 2.4 GHz. Measurement results of the circuit shows >76% efficiency at both bands. Further, the rectifier shows wide input power range with efficiency above 50%, which makes the circuit an attractive candidate for next-generation high power dual-band RF-DC energy harvester.

Acknowledgment

This work was supported in part by the U.S. National Science Foundation under Grants CNS-1564014 and CNS-1705026, in part by the Center for Design of Analog-Digital Integrated Circuits and in part by the Joint Center for Aerospace Technology Innovation.

References

[1] X. Lu, P. Wang, D. Niyato, D. I. Kim, and Z. Han, "Wireless Charging Technologies: Fundamentals, Standards, and Network Applications," *IEEE Commun. Surv. Tutor.*, vol. 18, no. 2, pp. 1413–1452, Secondquarter 2016.

[2] C. R. Valenta and G. D. Durgin, "Harvesting Wireless Power: Survey of Energy-Harvester Conversion Efficiency in Far-Field, Wireless Power Transfer Systems," *IEEE Microw. Mag.*, vol. 15, no. 4, pp. 108–120, Jun. 2014

[3] S. Abbasian and T. Johnson, "Power-Efficiency Characteristics of Class-F and Inverse Class-F Synchronous Rectifiers," *IEEE Trans. Microw. Theory Tech.*, vol. 64, no. 12, pp. 4740–4751, Dec. 2016.

[4] M. Roberg, T. Reveyrand, I. Ramos, E. A. Falkenstein, and Z. Popovic, "High-Efficiency Harmonically Terminated Diode and Transistor Rectifiers," *IEEE Trans. Microw. Theory Tech.*, vol. 60, no. 12, pp. 4043–4052, Dec. 2012.

[5] S. N. Ali, T. Johnson, and D. Heo, "DC Polarity Control in Radio Frequency Synchronous Rectifier Circuits," *IEEE Microw. Wirel. Compon. Lett.*, vol. 27, no. 12, pp. 1107–1109, Dec. 2017.

[6] M. Litchfield, S. Schafer, T. Reveyrand, and Z. Popovic, "High-efficiency X-Band MMIC GaN power amplifiers operating as rectifiers," in *2014 IEEE MTT-S International Microwave Symposium (IMS2014)*, Tampa, FL, USA, 2014, pp. 1–4.

[7] D. Wang and R. Negra, "Design of a dual-band rectifier for wireless power transmission," in *2013 IEEE Wireless Power Transfer (WPT)*, Perugia, Italy, 2013, pp. 127–130.

[8] F. You, S.-W. Dong, Y. Wang, X. Yu, and C. Li, "Design Method of Self-driving RF-DC Rectifier Based on Waveform-guided Solutions to Passive Matching Network," *IEEE Trans. Power Electron.*, pp. 1–1, 2018.